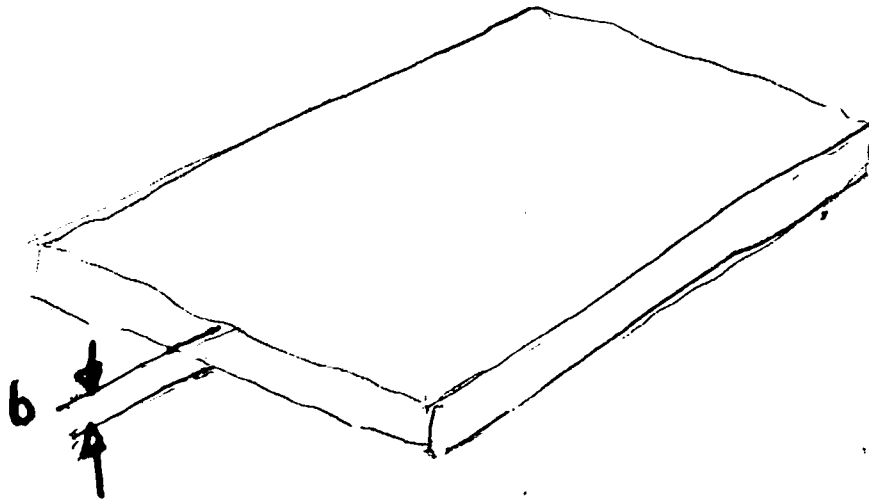


VISCOUS POTENTIAL FLOW ANALYSIS
OF RADIAL FINGERING IN A HELE-SHAW CELL

H. Kim, T. Fumada, D. D. Joseph



b is small
 $u(x, y)$ is the average of $u(x, y, z)$ over z

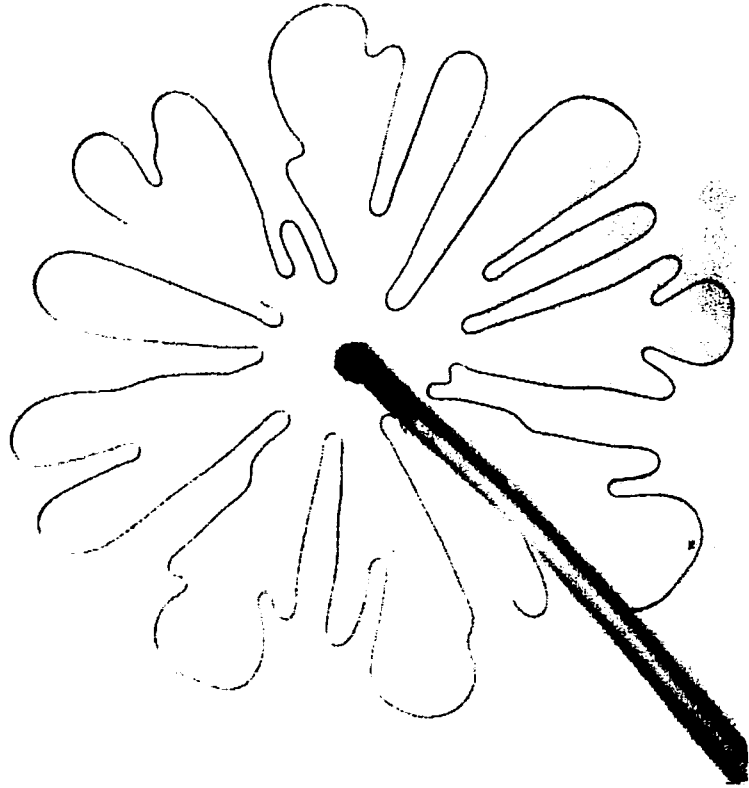


FIGURE 1. The pattern which occurs after the injection of air into a Hele Shaw cell filled with glycerine.

Injection of gas into liquid is unstable
Withdrawal of liquid from gas is unstable

BASIC FLOW (Paton)

Chuoque *et al.* (1959), Scheidegger (1960a, b) have made studies of the initial growth of fingers from a linear interface. In particular, Chuoque *et al.* have shown that surface tension prevents fingers from occurring below a certain wavelength, where wavelength is defined as peak-to-peak separation.

The problem of the instability of an initially circular interface has been examined elsewhere (Bataille 1968; Wilson 1975). Since the analysis is illustrative and beneficial to the subsequent analysis, a version of the derivation will be included here.

Darcy's law is the equation governing the velocity of flow v in a porous medium or a Hele Shaw cell as a function of pressure p ,

$$v = -M \nabla p, \quad (1)$$

where M is the fluid mobility. Mobility in a Hele Shaw cell is a function of the plate spacing b and the fluid viscosity μ :

$$M = b^2 / 12\mu. \quad (2)$$

In the problem under consideration, the subscripts 1 and 2 will be used to refer to the inner and outer fluids respectively. For incompressible flow, Darcy's law in polar co-ordinates leads to

$$\frac{\partial^2 \phi_j}{\partial r^2} + \frac{1}{r} \frac{\partial \phi_j}{\partial r} + \frac{1}{r^2} \frac{\partial^2 \phi_j}{\partial \theta^2} = 0, \quad (3)$$

where $\phi_j = M_j p_j$ is the velocity potential.

Part of a circular interface with a sinusoidal perturbation is shown in figure 2. The source has volume flow rate Qb and the circle has radius R , so that, for unperturbed displacements,

$$R(t) = (Q(t - t_0) / \pi)^{1/2}, \quad (4)$$

if $R = 0$ at $t = t_0$. For both inflow and outflow, $Q(t - t_0) > 0$. The velocity potential of the steady flow can be derived from (3) as

$$\phi_j^{(0)} = -\frac{Q}{2\pi} \left[\ln \frac{r}{R} + \frac{M_j}{M_2} \right], \quad (5)$$

which satisfies the continuity of pressure
and normal velocity at the interface

VPF

The pressure is not continuous

The normal stress is continuous

PERTURBED FLOW

L. Paterson

516

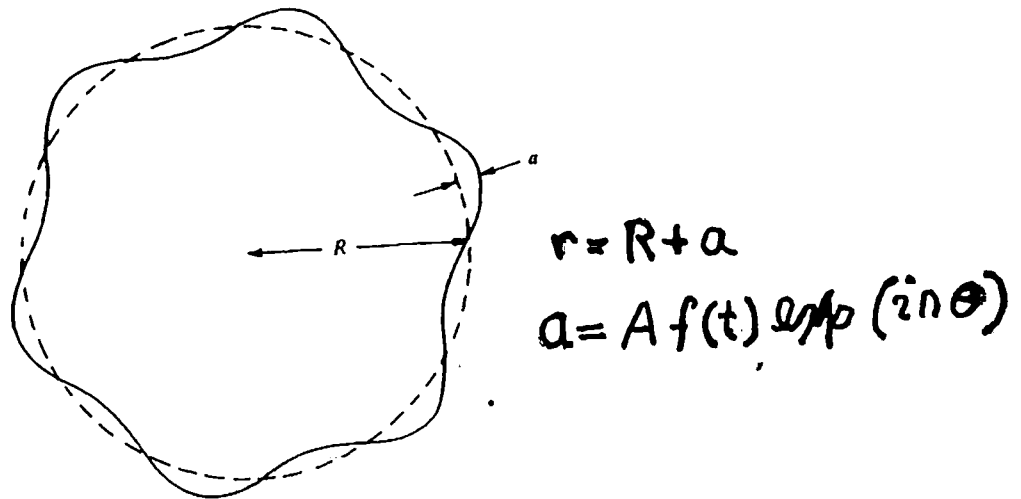


FIGURE 2. A circular interface of radius R with a wavelike perturbation a .

n is finger number - like the wave number

$$\phi_j = \phi_j^{(0)} + (-1)^j \beta \left(\frac{r^n}{R^n} \right)^{(-1)^j - 1} \exp(in\theta). \quad (7)$$

The condition of continuity at the perturbed interface (to first order at $r = R(t)$) determines β as

$$\beta = \frac{A}{n} \left(\frac{Qf}{2\pi R} + R \frac{df}{dt} \right) \quad (8)$$

The pressure drop across the interface depends on the surface tension σ through

$$p_1 - p_2 = \sigma \left(\frac{2}{b} + \frac{1}{R} - \frac{a + d^2 a / d\theta^2}{R^2} \right) \quad *$$

to first order, since $r = R + a$. Using (5)-(9) gives

$$\frac{1}{f} \frac{df}{dt} = \frac{Qn}{2\pi R^2} \left[\frac{M_1 - M_2}{M_1 + M_2} \right] - \frac{Q}{2\pi R^2} - \frac{\sigma n(n^2 - 1)}{R^3} \left[\frac{M_1 M_2}{M_1 + M_2} \right]. \quad (10)$$

If $M_1 \gg M_2$, (10) becomes

$$\frac{df}{dt} = \frac{n-1}{R^2} \left(\frac{Q}{2\pi} - \frac{n(n+1)\sigma M_2}{R} \right) f. \quad (11)$$

* VPF: the normal stress is balanced by surface tension

BASIC FLOW PRESENT WORK

The interface is given by $r = R(t)$, where the mean radius $R(t)$ satisfies

$$\pi R(t)^2 = \pi R_0^2 + Qt \text{ (injection), } \pi R(t)^2 = \pi R_0^2 - qt \text{ (withdrawal)}. \quad (2.7)$$

The velocity potential satisfies Laplace's equation and is given by

$$\phi_{01}(r, t) = -\frac{Q}{2\pi} (\text{Log}(r) - \text{Log}(R(t))) - \frac{Q}{2\pi} \frac{M_1}{M_2} + c_1, \quad (2.8)$$

$$\phi_{02}(r, t) = -\frac{Q}{2\pi} (\text{Log}(r) - \text{Log}(R(t))) - \frac{Q}{2\pi} + c_2. \quad (2.9)$$

The kinematic condition at the interface is given by

$$\frac{\partial R}{\partial t} = - \left(\frac{\partial \phi_{01}}{\partial r} \right)_{r=R}, \quad \frac{\partial R}{\partial t} = - \left(\frac{\partial \phi_{02}}{\partial r} \right)_{r=R} \quad (2.10)$$

$$c = c(t)$$

Then the pressure is given by

$$p_{01}(r, t) = \frac{\phi_{01}(r, t)}{M_1}, \quad p_{02}(r, t) = \frac{\phi_{02}(r, t)}{M_2}. \quad (2.11)$$

The normal stress balance is given by

$$p_{01}(R, t) + 2\mu_1 \left(\frac{\partial^2 \phi_{01}(r, t)}{\partial r^2} \right)_{r=R} - p_{02}(R, t) - 2\mu_2 \left(\frac{\partial^2 \phi_{02}(r, t)}{\partial r^2} \right)_{r=R} = \sigma \left(\frac{2}{b} + \frac{1}{R(t)} \right) \quad (2.12)$$

which provides the relation of c_1 and c_2 :

$$-\frac{c_2}{M_2} + \frac{c_1}{M_1} - \sigma \left(\frac{2}{b} + \frac{1}{R(t)} \right) + \frac{Q}{\pi R(t)^2} (\mu_1 - \mu_2) = 0. \quad (2.13)$$

VPF

The first part is the pressure difference, the second the interface tension, and the third is due to VPF. The equations for withdrawal are derived if Q is changed only to $-q$.

PETURBED FLOW VPF

$$\phi = \phi_0 + \phi_1$$

The normal stress balance for the perturbed field at $r = R + a(t, \theta)$ is given by

$$\begin{aligned} & p_{01} + 2\mu_1 \frac{\partial^2 \phi_{01}}{\partial r^2} - \left(p_{02} + 2\mu_2 \frac{\partial^2 \phi_{02}}{\partial r^2} \right) + p_{11} + 2\mu_1 \frac{\partial^2 \phi_{11}}{\partial r^2} - \left(p_{12} + 2\mu_2 \frac{\partial^2 \phi_{12}}{\partial r^2} \right) \\ &= \left[p_{01} + 2\mu_1 \frac{\partial^2 \phi_{01}}{\partial r^2} - \left(p_{02} + 2\mu_2 \frac{\partial^2 \phi_{02}}{\partial r^2} \right) \right]_{r=R} \\ &+ \left\{ \frac{\partial}{\partial r} \left[p_{01} + 2\mu_1 \frac{\partial^2 \phi_{01}}{\partial r^2} - \left(p_{02} + 2\mu_2 \frac{\partial^2 \phi_{02}}{\partial r^2} \right) \right] \right\}_{r=R} a \\ &+ \left[p_{11} + 2\mu_1 \frac{\partial^2 \phi_{11}}{\partial r^2} - \left(p_{12} + 2\mu_2 \frac{\partial^2 \phi_{12}}{\partial r^2} \right) \right]_{r=R} + O(a^2) \\ &= \sigma \left(\frac{2}{b} + \frac{1}{R(t)} - \frac{a}{R(t)^2} - \frac{1}{R(t)^2} \frac{\partial^2 a}{\partial \theta^2} + O(a^2) \right), \end{aligned} \quad (2.21)$$

which is then arranged, after using (2.12), as

With $\mu_1 = b^2/(12M_1)$ and $\mu_2 = b^2/(12M_2)$, VPF equation (2.25) gives

$$\begin{aligned} & -\frac{(n^2 - 1)\sigma}{R(t)^2} - \frac{b^2 [M_1(n-1) + M_2(n+1)]}{12M_1 M_2 \pi R(t)^3} Q + \frac{M_1(n-1) - M_2(n+1)}{2M_1 M_2 n \pi R(t)} Q \\ &= \left(\frac{b^2 [M_2(n-1) + M_1(n+1)]}{6M_1 M_2 R(t)} + \frac{(M_1 + M_2)R(t)}{M_1 M_2 n} \right) \frac{f'(t)}{f(t)}. \end{aligned} \quad (2.26)$$

VPF \rightarrow PATERSON

$$b=0$$

6

HADAMARD INSTABILITY. Viscosity and surface tension stabilize short waves $\lambda = \frac{2\pi}{n}$

To investigate the effects of VPF terms proportional to b^2 , consider the case $\sigma = 0$ when the finger number $n \gg 1$. In this case

$$\frac{f'(t)}{f(t)} = -\frac{b^2 n^2 (M_1 + M_2) + 6n (M_2 - M_1) R(t)^2}{b^2 n^2 (M_2 + M_1) + 6(M_1 + M_2) R(t)^2} \frac{Q}{2\pi R(t)^2} \quad (2.27)$$

When $n \rightarrow \infty$

$$\frac{f'(t)}{f(t)} \rightarrow -\frac{Q}{2\pi R(t)^2} \quad (2.28)$$

The VPF terms are stabilizing. On the other hand, when $b^2 = 0$

$$\frac{f'(t)}{f(t)} = -\frac{n (M_2 - M_1) Q}{(M_2 + M_1) 2\pi R(t)^2} > 0, \quad (2.29)$$

so that large finger numbers are unstable and since $f'/f \propto n$ they are *Hadamard unstable*; large finger number fingers grow without limit for any time no matter how small, as $n \rightarrow \infty$.

We think that this is new

2.3 Explicit formula for the perturbed interface

We may transform t to R :

$$\frac{df(t)}{dt} = \frac{dR}{dt} \frac{df(R)}{dR} = \frac{Q}{2\pi R} \frac{df(R)}{dR}, \quad (2.31)$$

thus $0 \leq t < \infty$ is converted to $R_0 \leq R < \infty$. Equation (2.26) can be written with (2.27) and is integrated as

$$\begin{aligned} \text{Log} \left(\frac{f(R)}{f(R_0)} \right) &= \int_{R_0}^R \frac{f'(R)}{f(R)} dR \\ &= - \frac{2\pi\sigma M_1 M_2 (n^3 - n)}{bQ\sqrt{(M_1 + M_2)(M_2(n^2 - n) + M_1(n^2 + n))}/6} \left[\text{ArcTan} \left[\frac{\sqrt{6(M_1 + M_2)}R}{b\sqrt{M_2(n^2 - n) + M_1(n^2 + n)}} \right] \right. \\ &\quad \left. - \text{ArcTan} \left[\frac{\sqrt{6(M_1 + M_2)}R_0}{b\sqrt{M_2(n^2 - n) + M_1(n^2 + n)}} \right] \right] \\ &\quad - \frac{M_2(n+1) + M_1(n-1)}{M_2(n-1) + M_1(n+1)} \text{Log}[R/R_0] \\ &\quad + \frac{M_1^2(n+2)(n-1) - 2M_1M_2n - M_2^2(n-2)(n+1)}{2(M_1 + M_2)((n-1)M_2 + (n+1)M_1)} \\ &\quad \times \text{Log} \left[\frac{6(M_1 + M_2)R^2 + M_2(n^2 - n) + M_1(n^2 + n)}{6(M_1 + M_2)R_0^2 + M_2(n^2 - n) + M_1(n^2 + n)} \right]. \end{aligned} \quad (2.32)$$

8

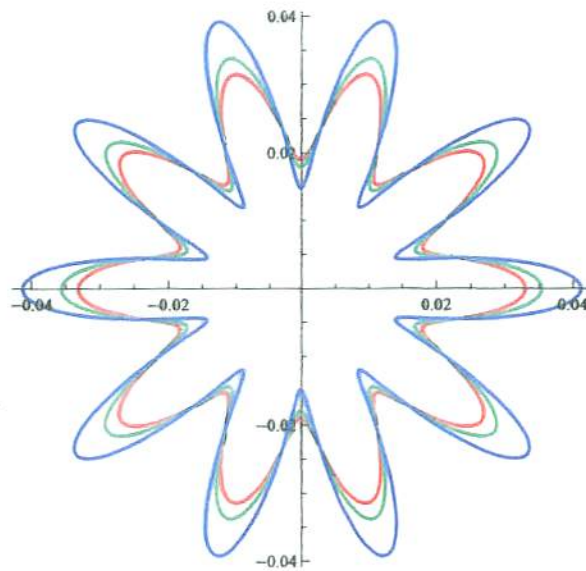


Fig.4b Finger pattern for $data1 = (\mu_2, \sigma, M_1, M_2, P_I) = 0.001, 0.00109649, 0.0000208333, 0$ and $n = 10$.
 $r_1 = 0.026$ (red), $r_1 = 0.0267$ (green), $r_1 = 0.028$ (blue).

Table xx Lower cut-off ($n = 1$) and the first instability at $n = 2$.

ξ	R	VPF				Paterson			
		n_m	α_m	n_c	α_c	n_m	α_m	n_c	α_c
50	0.025			1	-0.0000149156			1	-0.0000149166
100	0.05			1	-3.72909×10^{-6}			1	-3.72915×10^{-6}
200	0.1	2	0.0000109956	3	-1.35492×10^{-6}	2	0.0000109961	3	-1.35435×10^{-6}

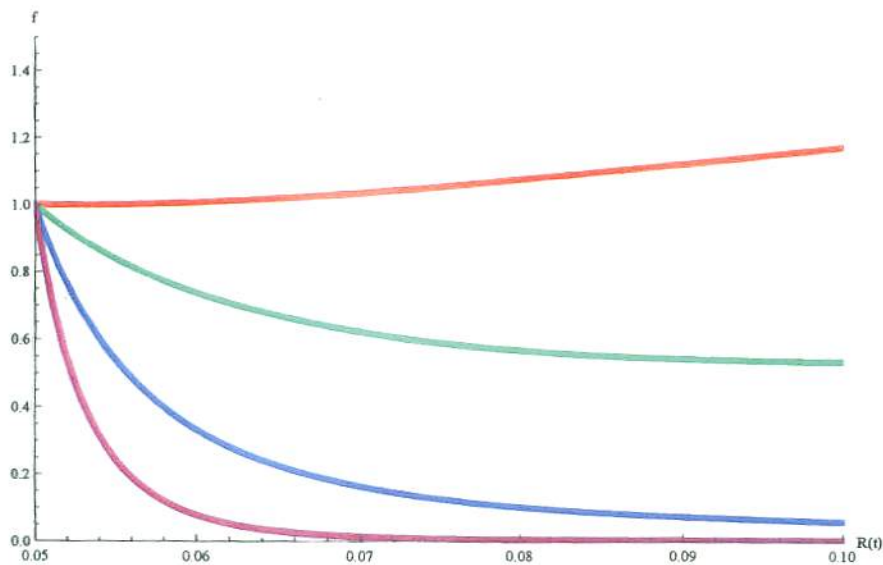


Fig.5 $f(R)$ versus R for $n = 2$ (red), $n = 3$ (green), $n = 4$ (blue), $n = 5$ (magenta). VPF with
 $data1 = (\mu_2, \sigma, M_1, M_2, P_I) = (0.001, 0.063, 0.00109649, 0.0000208333, 16.4934)$.

9

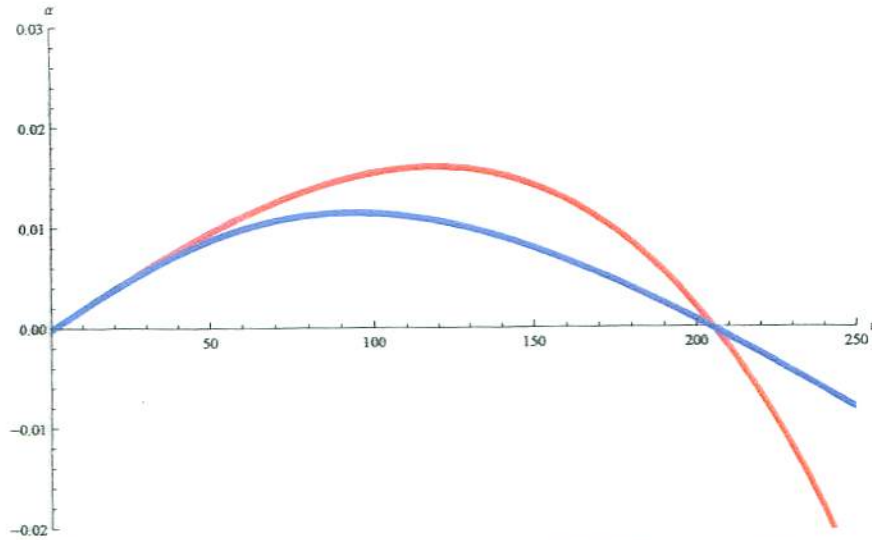


Fig.2b Growth rate α versus n for $(P_I, m, \xi, R) = (0.00164934, 1.9 \times 10^{-6}, 70., 0.035)$.

Table 1 Maximum growth rate α_m given at $n = n_m$ and cut-off n_c at which α_c becomes negative, for various values ξ . (SO10000-air)

ξ	R	VPF				Paterson			
		n_m	α_m	n_c	α_c	n_m	α_m	n_c	α_c
50	0.025	75	0.017309	173	-0.000103003	101	0.0264067	174	-0.000307776
60	0.03	85	0.0138616	190	-0.000124814	110	0.0201153	191	-0.000426242
70	0.035	94	0.0114481	205	-0.0000341013	119	0.0159789	206	-0.000197903
20	0.01	37	0.049297	108	-0.000715806	64	0.103467	110	-0.00188615
40	0.02	64	0.0225756	154	-7.8159×10^{-6}	90	0.0368402	156	-0.000958135

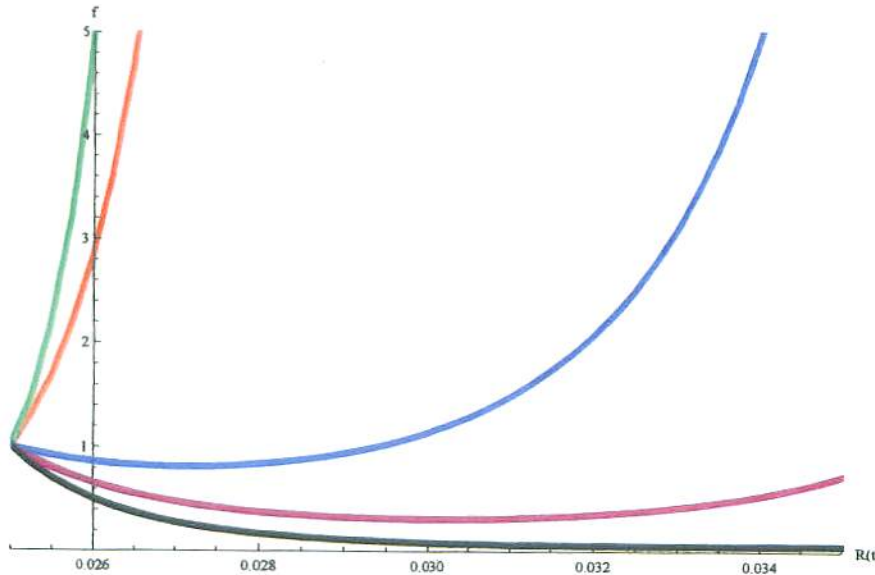


Fig.3 $f(R)$ versus R for $n = 30$ (red), $n = 100$ (green), $n = 180$ (blue), $n = 190$ (magenta), $n = 200$ (black). VPF with $data1 = (\mu_2, \sigma, M_1, M_2, P_I) = (10, 0.063, 0.00109649, 2.08333 \times 10^{-9}, 0.00164934)$.

5 The case $M_2 \ll M_1$

When $M_1 \gg M_2$, (2.26) reduces to

$$-(n-1) \frac{b^2 n Q + 12 M_2 \pi \sigma R(t) (n^2 + n) - 6 Q R(t)^2}{2 \pi R(t)^2 (b^2 (n^2 + n) + 6 R(t)^2)} = \frac{f'(t)}{f(t)}, \tag{5.1}$$



Fig.1a n_m versus $\xi = R/b$ for $P_I = 0.01$ (Paterson's case given by (3.16)).

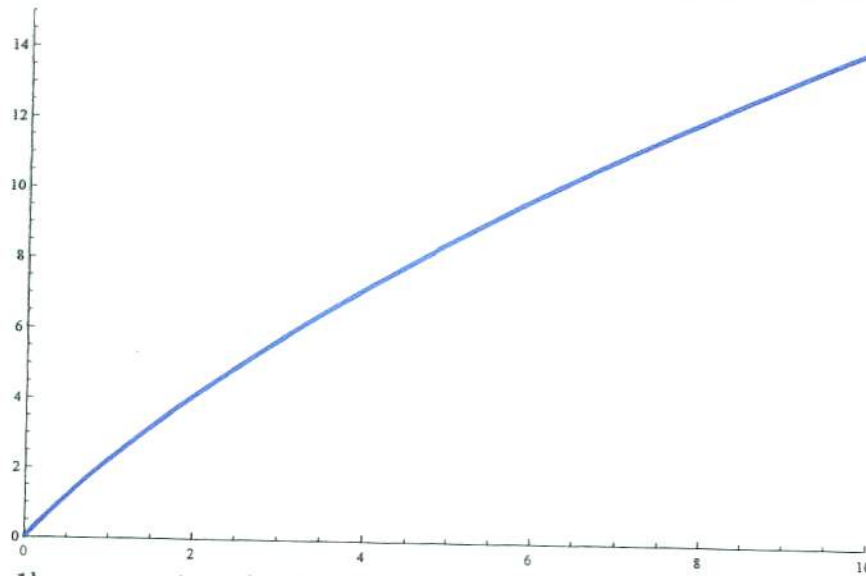


Fig.1b n_m versus $\xi = R/b$ for $P_I = 0.01$ (VPF). Present case given by n_m of (3.14).

4 Numerical results comparing Paterson and VPF

The maximum growth rate of VPF is different from that of Paterson's case, for SO1000-air.

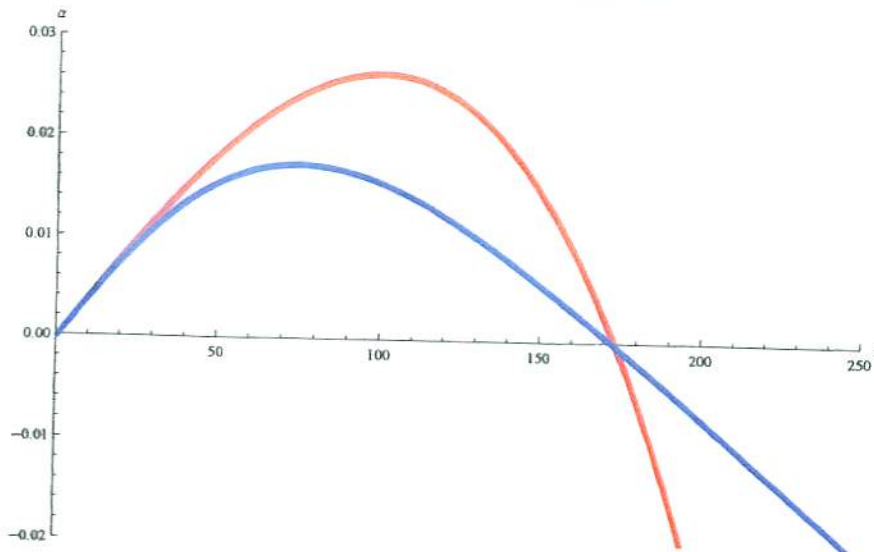


Fig.2a Growth rate α versus n for $(P_I, m = \mu_1/\mu_2, \xi = R/b, R) = (0.00164934, 1.9 \times 10^{-6}, 50., 0.025)$.

11